

Available online at www.sciencedirect.com

ScienceDirect

www.elsevier.com/locate/jes

JES
 JOURNAL OF
 ENVIRONMENTAL
 SCIENCES
www.jesc.ac.cn

Transient species in the ozonolysis of tetramethylethene

Xiaolu Yang¹, Jianguo Deng², Dong Li¹, Jianhua Chen^{1,*}, Yisheng Xu¹, Kai Zhang¹, Xiaona Shang¹, Qing Cao¹

¹State Key Laboratory of Environmental Criteria and Risk Assessment, Chinese Research Academy of Environmental Sciences, Beijing 100012, China

²School of Environment, Tsinghua University, Beijing 100084, China

ARTICLE INFO

Article history:

Received 29 September 2019

Revised 12 February 2020

Accepted 17 March 2020

Available online 30 April 2020

Keywords:

Tetramethylethylene

Ozone

Criegee mechanism

Matrix isolation

Quantum chemical calculations

ABSTRACT

The reaction of alkenes with ozone has great effect on atmospheric oxidation, its transient species can produce OH radicals and contribute to the formation of secondary organic aerosols (SOA). In the present study, the reaction of tetramethylethene (TME) with ozone was investigated using self-assembled low temperature matrix isolation system. The TME and ozone were co-deposited on a salt plate at 15 K, and then slowly warmed up the plate. The first transient species primary ozonide (POZ) was detected, indicating that the reaction followed Criegee mechanism. Then POZ began to decompose at 180 K. However, secondary ozonide (SOZ) was not observed according to Criegee mechanism. Probably, Criegee Intermediate (CI) did not react with inert carbonyl of acetone, but with remaining TME formed tetra-methyl epoxide (EPO).

© 2020 The Research Center for Eco-Environmental Sciences, Chinese Academy of Sciences. Published by Elsevier B.V.

Introduction

Alkenes, from natural and anthropogenic sources, are important components of tropospheric volatile organic compounds (VOCs), and their reaction with ozone is a major way for alkene reduction (Hoffmann et al., 1998). In the troposphere, alkenes rapidly react with ozone, which could influence the atmospheric chemical processes in two ways. First, ozonolysis can produce OH radicals, the most important oxidant which determines the lifetime of other substances in the atmosphere (Feltham et al., 2000). Second, ozonolysis can be one of secondary organic aerosol (SOA) sources, which causes deterioration of visibility and air quality (Laura et al., 2019).

On the basis of current knowledge, Criegee mechanism is a widely accepted reaction mechanism of alkenes with ozone, which proposes a very important intermediate, the carbonyl

oxide, defined as Criegee intermediate (CI) (Giorio et al., 2017). The Criegee mechanism can be described simply in three steps (Fig. 1): (1) Ozone undergoes 1,3dipolar cycloaddition to the alkene double-bond and forms the primary ozonide (POZ), 1,2,3-trioxolane (Baley et al., 1978). (2) POZ is decomposed into a molecule of carbonyl oxide (CI), and a molecule of aldehyde or ketone. (3) Secondary ozonides (SOZ) is formed by the recombination of individual aldehyde/ketone and carbonyl oxide molecules.

CI is an active intermediate and plays an important role in atmospheric chemistry. As mentioned above, CI can react with species like H₂O, NH₃, SO₂, and carboxylic acid, and produce OH radical or SOA (Rabi et al., 2019; Roussou et al., 2019; Wang et al., 2019; Jani et al., 2018). Also, CI can isomerize to unsaturated hydrogen peroxide by itself and contribute to atmospheric chemistry. Up to now, the direct observation of CI was not successful due to its high reactivity, and the knowledge of CI is still limited. Recent researches showed that CI was observed in the atmosphere, by using 5,5-dimethyl-1-pyrroline N-oxide (DMPO) to react with it to form a stable derivative and then detected

* Corresponding author.

E-mail: chenjh@craes.org.cn (J. Chen).

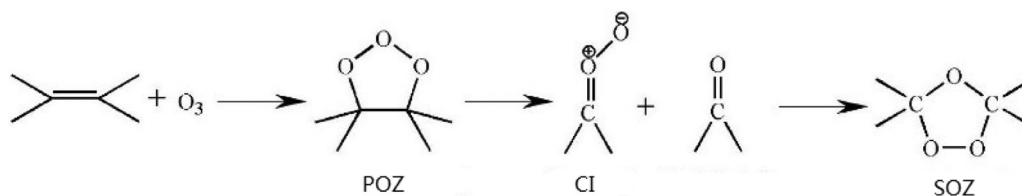


Fig. 1 – Criegee mechanism of the reaction of alkenes with ozone (Criegee, 1975).

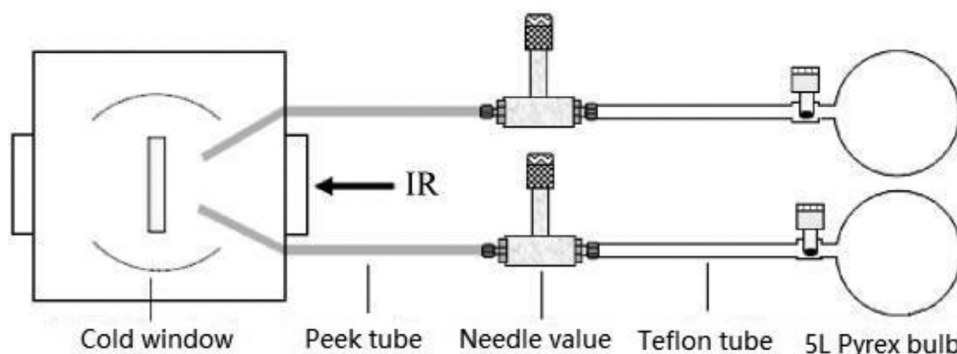


Fig. 2 – Twin jet deposition setup of ozone and alkenes. IR: infrared radiation.

by proton transfer reaction-mass spectrometry (PTR-MS) (Giorio et al., 2017).

Tetramethylethene (TME) can be as a good model species to study CI due to its highly symmetrical structure. Theoretically, the POZ generated by the reaction of ozone and TME should be equivalent to the intermediates generated by Criegee mechanism, both being with only one kind of structure, which makes the reaction process relatively simple. Niki et al. (1987) studied the reaction in gas-phase and found that the stoichiometric ratio of TME to ozone is about 1.7, which was much higher than that of other kinds of alkene-ozone reactions. It was speculated that the CI $((\text{CH}_3)_2\text{COO}$ radical) quickly isomerized into unsaturated hydrogen peroxide, then the latter decomposed to OH radicals and $\text{CH}_3\text{C}(=\text{O})\text{CH}_2$ radicals. The continual reaction of OH radical with TME could account for the high stoichiometric ratio. Hull et al. (1972) cooled TME and ozone together by liquid N_2 , then slowly warmed up the reactants and found that the transient species POZ was observed not SOZ. SOZ was supposed to be not generated due to the inertness of acetone carbonyl. However, Epstein et al. (2008) investigated the reaction of TME and ozone in condensed phase again by method similar with Hull's, and detected the SOZ of TME. So the existence of SOZ is still controversial and the reaction of TME and ozone is still far from being well-understood.

Low-temperature matrix isolation technology is a powerful method for the research of reaction intermediates (Kugel et al., 2015; Lv et al., 2017; Tang et al., 2017). The inert matrix isolates the reactive intermediates by inert atoms or molecules, meanwhile, low temperature can reduce the reactivity of active intermediates and prolong their residence time (Jussi et al., 2018; Krupa and Wierzejewska, 2016). In the present study, a self-established matrix isolation system was used combining with the heating program to re-examine the reaction of ozone and TME. Fourier infrared spectrometer was adopted to detect the transient species such as POZ, SOZ and CI.

1. Materials and methods

1.1. Experimental materials

Tetramethylethene (99%, Zhengyuan chemical industry company, China) was used directly as received. Argon (99.9992%, Zhengyuan chemical industry company, China) was used as the matrix gas without further purification. Ozone was generated by a Tesla coil discharge of O_2 (99.9960%, Zhengyuan chemical industry company, Beijing) and purified by liquid N_2 . A self-established matrix isolation device was utilized in the experiment (Deng et al., 2012a; Chen et al., 2013), mainly consisted of five parts, including refrigerating system, vacuum system, temperature controlling system, air distribution system and detecting system. In general, the matrix isolation equipment used in the experiment was a conventional matrix isolation apparatus based on a closed-cycle helium refrigerator (APD Cryogenics model DE-204NE, Sumitomo, USA). The high vacuum (10^{-7} mbar) was maintained by a turbomolecular pump with an oil diffusion backing pump. The temperature of the CsI window was controlled by a Lake Shore Cryogenics temperature controller (model 331, Lakeshore, USA). In the detection system, a model of an 80 v vacuum Fourier transform infrared (FTIR) spectrometer (Bruker, Germany) was used. Ozone and tetramethylethene were mixed separately with Ar to the desired ratio (Mixed-gas/Ar = 1:100) in a 5 L Pyrex bulb (Fig. 2). The peek tube and the cold window were evacuated (about 10^{-5} Pa) with the temperature gradually dropping to 15 K and kept constant. The ozone/Ar and alkene/Ar were co-deposited (in a ratio of 2 mmol/hr) onto a cold window (15 K) from two separate lines. After 2hr of deposition, the infrared spectra of the sample were scanned. Meanwhile, the matrix was annealed to 35 K and held at this temperature for 1 hr (Deng et al., 2012b). During the process, the matrix solids softened and the Ar atoms began to diffuse. Then it was further heated to 40 K, and Ar started to evapo-

rate rapidly. All Ar matrix on the cold window evaporated at 55 K. Although some of the reactants were carried away by the Ar gas, most of the reactants remained on the cold window to form a neat film due to the high melting and boiling point of ozone and TME. Finally, we turned off helium refrigerator and slowly warmed up the salt plate. The infrared spectrum of the obtained neat film was recorded for every 10 K until the cold window was slowly annealed to room temperature.

1.2. Calculation details

The theoretical calculations of the transient species like POZ, SOZ and CI were performed on the supercomputer (SGI 4700, Lepnitz computing center of Munich, Germany) with the software of Gaussian 03 suite programs at the information center of the Chinese Research Academy of Environmental Sciences (CRAES). The high-base group 6–311++G(2d,2p) of the B3LYP hybridization function of density functional theory (DFT) was selected for optimization structure of the transient species in this research, and the calculated vibration frequency of the transient species was used to being compared with experiment values.

2. Results and discussion

2.1. Infrared spectra analysis

The infrared spectra of obtained products were recorded as the temperature increased. Variations mainly occurred at 600–1900 cm^{-1} (Fig. 3a). Co-deposition of ozone and TME at 15 K produced a series of new peaks (i.e., 650, 684, 723, 851, 953, 1093, 1143, 1200, 1226, 1235, and 1707 cm^{-1}) compared to the blank spectra, indicating that a reaction occurred and produced a new product. When the temperature was raised to 60 K, all the peaks in the whole spectra were slightly increased, which was caused by the softening of the matrix solids (Frisch et al., 2004). As the neat film continues to be heated up, the intensity of the peaks belonging to reactants TME and ozone gradually decreased. However, the intensity of the peaks belonging to the products increased, indicating that the reaction continued. At 110 K, the absorption peaks of ozone disappeared (Fig. 3b). The reaction of TME and ozone was over. The product peaks did not change significantly before 170 K.

From 170 K, the absorption peaks of the products (i.e., 650, 684, 723, 851, 867, 953, 1147, 1152, 1200, 1226, 1370, and 1389 cm^{-1}) began to decline and disappeared at 180 K (Fig. 3c). Meanwhile, additional new peaks were formed at 975, 845, 1180, 1206, 1378, and 1460 cm^{-1} . What's more, some already existing peaks at 1707, 1235, and 1093 cm^{-1} increased profoundly at 180 K.

When the temperature is continued to rise, no significant change occurred again throughout the IR spectrum. When the temperature of the cold window was close to room temperature, all the absorption peaks gradually disappeared and the substance evaporated from the plate.

2.2. Quantum chemical calculation method to verify experimental results

The new peaks were produced after co-deposited of ozone and TME, indicating that the reaction of ozone and TME was rapidly performed before the salt plate. TME being with the lowest activation energy among all alkenes was prone to react with ozone was prone to react with ozone, which is the cause of the occurrence of reaction. The new peaks (684, 723, 851, 953, 1147, 1152, 1200, 1226, 1370 and 1389 cm^{-1}) were assigned to the primary oxides (POZ) according to Criegee mechanism.

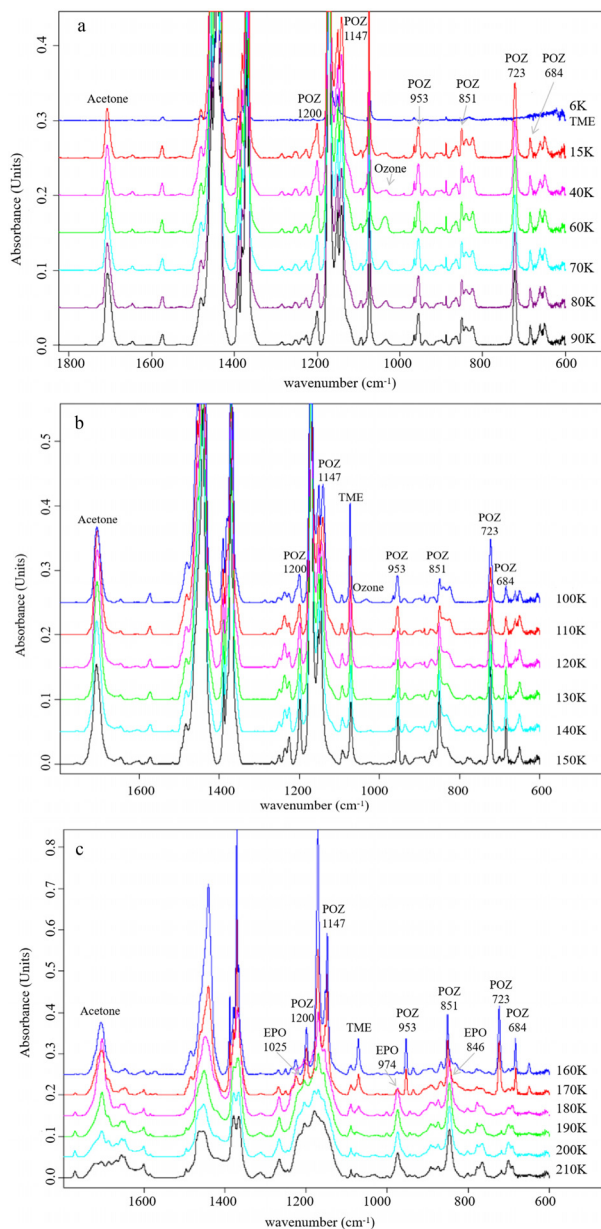


Fig. 3 – Infrared spectra of a matrix formed by twin jet deposition of tetramethylethene and ozone after annealing from (a) 15 to 90 K, (b) 100 to 150 K and (c) 160 to 210 K. POZ: primary ozonide; SOZ: secondary ozonide; EPO: epoxide.

The POZ peaks observed in our experiments were compared with Hull's and Epstein's in their experiment, and the theoretical calculations of IR absorption peak predicted by Gaussian 03 at B3LYP 6–311++G(2d,2p) level.

Hull et al. (1972) has firstly observed three peaks at 682, 721, and 854 cm^{-1} in the ozonolysis of TME, and attributed these peaks to TME POZ. Samuni et al. (1998) has observed three peaks at 691, 729, and 854 cm^{-1} in their research of ozone reaction with TME. And Epstein et al. (2010) has also found the three peaks are at 685, 725, and 852 cm^{-1} . In this study, the same three peaks were observed at 684, 723, and 851 cm^{-1} .

As shown in Table 1, the most intense vibration of TME POZ calculated by Gaussian 03 was OOO anti-symmetric stretching vibration, and the frequency was 772 cm^{-1} , which

Table 1 – Observed absorption by experiment and calculated vibrational frequency of tetramethylethene primary ozonide at B3LYP 6–311++G(2d,2p) level.

Experimental absorption peak					Theoretical calculation		Assignment
This study (cm ⁻¹)	Normalized absorbance (unit) ^a	Samuni et al., 1998 (cm ⁻¹)	Hull et al., 1972 (cm ⁻¹)	Epstein and Donahue, 2010 (cm ⁻¹)	Vibrational frequency (cm ⁻¹)	Intensity (km/mol)	
684	0.2	691	682	685	700	7	δ O–O–O
723	0.5	729	721	725	772	36	ν O–O–O as
851	0.4	854	852	852	867	16	Ring deform
953	0.2	950	953		957	7	
1147	1.0	1146	1148		1167	30	ν C–O s
1152	0.6	1150			1180	13	ν C–O as
1200	0.4	1196	1197		1222	23	δ O–C–C
1226	0.2	1261			1262	6	ν C–O s
1370	0.8		1370		1412	23	δ CH ₃
1389	0.3	1394			1419	9	δ CH ₃

ν: stretching vibration; as: anti-symmetric; δ: bending vibration; s: symmetric.

^a Normalized by the most intense absorption at 1147 cm⁻¹ in this work.

Table 2 – Observed absorption by experiment and calculated vibrational frequency of tetramethylethene secondary ozonide at B3LYP 6–311++G(2d,2p) level.

Experimental absorption peak					Theoretical calculation		Assignment
This study (cm ⁻¹)	Normalized absorbance (unit) ^a	Epstein and Donahue, 2010 (cm ⁻¹)	Griesbaum et al., 1989 (cm ⁻¹)	Normalized absorbance (unit) ^b	Vibrational frequency (cm ⁻¹)	Intensity (km/mol)	
846	0.8	845	845	0.3	859	31	ν C–O–C s
974	0.7	975	876	0.2	933	3	Ring deform
			1 005	0.7	1009	119	ν C–O–C as
1180	1.0		1115	0.1	1136	8.3	Ring deform
1205	0.8	1208	1215	1.0	1225	241	ν O–C–O s
			1245	0.4	1233	47	ν O–C–O as
			1265	0.2	1258	71	ν C–C–C as
1378	0.9		1375	0.6	1407	55	δ CH ₃ s
1463	0.7		1470	0.1	1485	3	δ CH ₃ as

^a Normalized by the most intense absorption at 1147 cm⁻¹ in this study.

^b Normalized by the most intense absorption at 1215 cm⁻¹ in this study.

corresponded to the peak at 723 cm⁻¹ observed at the low frequency region. Another characteristic vibration of POZ were calculated to be OOO bending and CO bending vibrations at 700 and 867 cm⁻¹, corresponding to the absorption peaks observed at 684 and 851 cm⁻¹ in this experiment.

As the temperature raised to 110 K, the neat film became soft. Ozone and TME can move slowly and react with each other, resulting in an increase in the intensity of the POZ peaks. With temperature continued to rise to 180 K, the peaks belonging to the POZ rapidly decreased and disappeared, indicating that the POZ began to split. After splitting the POZ, some new peaks appeared at 845, 975, 1206, 1378, and 1460 cm⁻¹. The Criegee mechanism believed that these new peaks should be associated with SOZ. Epstein et al (2010) also observed three new peaks at 845, 975, and 1208 cm⁻¹ after POZ decomposed, and attributed these three peaks to TME SOZ.

Similarly, the IR absorption spectrum of TME SOZ was calculated by Gaussian 03 and compared with the peaks observed after POZ decomposition in this study. As showed in Table 2, the strongest vibration of TME SOZ was the OCO symmetric stretching vibration. The absorption frequency should be 1225 cm⁻¹ with the greatest absorption intensity of

241 km/mol. However, the peak at 1206 cm⁻¹ observed in this study and peak at 1208 cm⁻¹ in Epstein's study after POZ decomposed are not the strongest. The second calculated strong vibration was COC anti-symmetric stretching vibration, with frequency of 1009 cm⁻¹ and intensity of 119 km/mol. However, no peaks were observed in nearby region in this study and Epstein's. The peaks of 1000 to 1300 cm⁻¹ were slightly crowded and it was difficult to exclude SOZ. In contrast, 846 and 975 cm⁻¹ were clearly observed in both experiments. The peak of 846 cm⁻¹ was higher than peak of 975 cm⁻¹. But the calculated peaks of the region cannot match with the peaks of 846 and 975 cm⁻¹, regardless of the location or intensity.

Griesbaum et al. (1989) and Sang and Kwan (1996) have successfully synthesized SOZ on the surface of Teflon and the peaks in their study were used to compare. As showed in Table 2, the peaks observed in Epstein's study and in this study are very different from the peaks in Griesbaum's work. However, the peaks in the Griesbaum's study were well matched to the calculated SOZ absorption peaks. Therefore, Griesbaum did obtain the absorption peak of TME SOZ. But the absorption peaks at 846, 974, and 1206 cm⁻¹ observed both in this study and same peaks in Epstein's study were

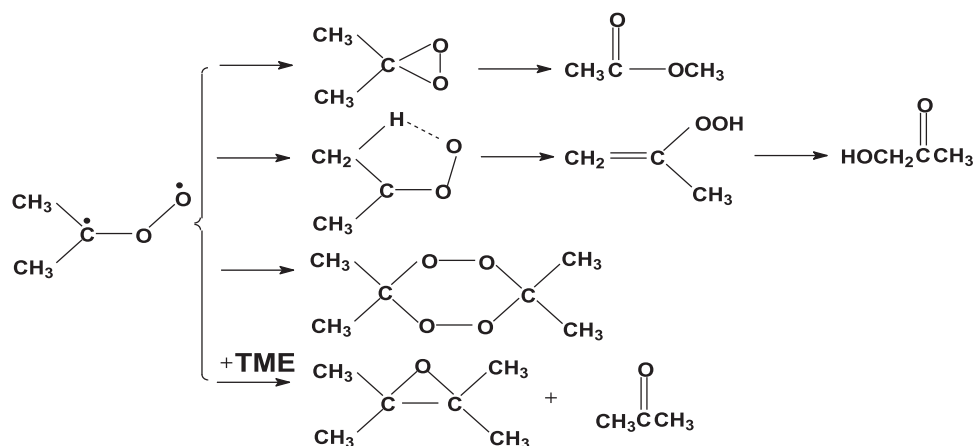


Fig. 4 – Reaction of tetramethylethene (TME) and ozone to produce a possible reaction channel for Criegee intermediate (CI).

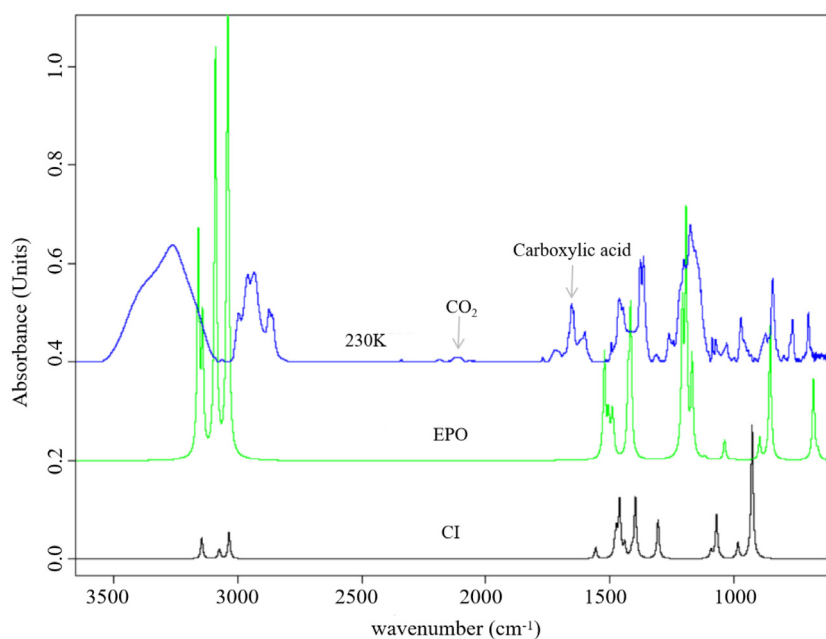


Fig. 5 – Comparisons of spectra of the reaction of TME and ozone at 230 K with theoretical spectra of tetramethyl EPO and CI.

not from TME SOZ. According to the acetone spectrum in Ar matrix at 35 K, the peaks at 1707, 1235, and 1093 cm^{-1} were associated with acetone. When POZ was decomposed, these acetone absorption peaks increased profoundly, suggesting that acetone was produced at a high yield. If TME SOZ was generated in the reaction, a large amount of acetone would not be generated, thus indirectly suggesting that the secondary ozonide (SOZ) was not produced according to Criegee mechanism after POZ decomposed.

As discussed and shown below, these 846, 974, and 1206 cm^{-1} peaks also impossibly correspond to the symbiotic $(\text{CH}_3)_2\text{COO}$ radical, i.e. Criegee Intermediate (CI), since the future of CI is O-O vibration with frequency nearby 928 cm^{-1} . Therefore, the CI was not detected in this study. If acetone did not react with CI to form TME SOZ, the possible reaction channels for the $(\text{CH}_3)_2\text{COO}$ radical are shown in Fig. 4.

$(\text{CH}_3)_2\text{COO}$ radical can be isomerized to dimethyldioxane. Murray et al. (1985) have successfully synthesized dimethyl-

dioxy heterocyclic propane by mixing carloate with acetone solution and measured two strong absorption peaks at 899 and 1209 cm^{-1} . Although the peak at 1209 cm^{-1} could correspond to the one at 1205 cm^{-1} in this experiment, there is no strong absorption peak near 900 cm^{-1} , indicating that no dimethyldioxane existed in this process. Then dimethyldioxane might be further isomerized to methyl acetate, and its $\text{C}=\text{O}$ stretch vibration absorption peak was at 1760 cm^{-1} and the stretching vibration absorption peak of C-O was at 1246 cm^{-1} . However, in the carbonyl region of the infrared spectra only the absorption peak of acetone was at 1707 cm^{-1} , with the absorption peak of weak formaldehyde at 1720 cm^{-1} , and peak of formic acid at 1770 cm^{-1} . Hence, the existence possibility of absorption peak of methyl acetate was excluded in the process.

$(\text{CH}_3)_2\text{COO}$ radical might also be isomerized to isopropenyl hydrogen peroxide, which has a strong $\text{C}=\text{C}$ double bond and end-allyl surface oscillations near 900 cm^{-1} . Neither

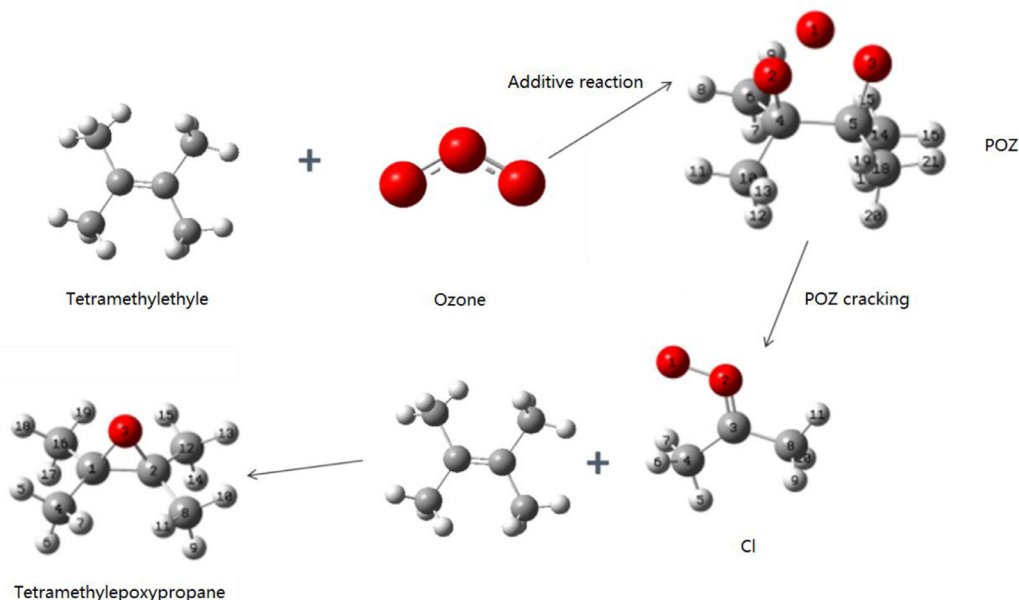


Fig. 6 – Formation mechanism of transient species by the reaction of ozone and TME. Red balls: oxygen atom; Gray balls: carbon element; White balls: hydrogen atom.

strong absorption peak of C=C double bond nor strong absorption peak at 900 cm^{-1} were detected, meaning that isopropenyl hydrogen peroxide was ruled out. Isopropenyl hydrogen peroxide can further isomerized to hydroxyl acetone. Sharma et al. (2008) have systematically studied the structure and infrared absorption peak of hydroxyl acetone in Ar matrix. The hydroxyl acetone has a strong C=O stretching vibration absorption peak at 1730 cm^{-1} , and the OH stretching vibration absorption peak was at 3505 cm^{-1} , the COH bending vibration absorption was at 1286 cm^{-1} , and the C–O was at 1103 cm^{-1} . None of the absorption peaks observed in this experiment can correspond to them, thus the possibility of producing hydroxyl acetone was eliminated.

The possibility of producing $(\text{CH}_3)_2\text{COO}$ dimer or polymers has been ruled out by Epstein since no corresponding absorption peak of strong OO stretching vibration was discovered in the spectra.

In early study of synthesis of dimethyldioxane, 90% of TME was found to be oxidized by dimethyldioxane to tetramethyl epoxypropane (Murray et al., 1985; Hinrichs et al., 1979). In this study, the absorption peak of the original reactant TME was not reduced to zero when TME POZ decomposed. Therefore, tetramethyl epoxypropane was expected to be generated from reaction of $(\text{CH}_3)_2\text{COO}$ radical (Criegee Intermediate, CI) with TME. Without IR absorption of EPO was measured ever before, so theoretically calculated absorption peak of tetramethyl epoxypropane was then compared to the measured spectrum at 230 K (Fig. 5).

Theoretical infrared spectra of EPO were agreed with the spectrum taken at 230 K as for bulk of substance are EPO at this moment. As showed in Fig. 5, theoretically calculated CCC symmetric stretching vibration at 1159 cm^{-1} corresponded well to the highest peak at 1180 cm^{-1} in this study. Then CCC anti-scaling vibration was calculated at 1174 cm^{-1} , which corresponded to the characteristic peak at 1205 cm^{-1} in the experiment. The symmetric and anti-symmetric bending vibration of CH_2 calculated at 1377 and 1474 cm^{-1} were corresponding to the peaks at 1378 and 1463 cm^{-1} . In addition, the C–O symmetric stretching vibration at 834 cm^{-1} corresponded well to another characteristic peaks observed at 846 cm^{-1} .

Therefore, it was concluded that EPO was produced after splitting of TME POZ. Of course, future works are needed to further verify the formation of epoxide in ozonolysis of TME, such as using the isotope labeled $^{18}\text{O}_3$ to react with TME.

Finally, the overall reaction process was shown in Fig. 6, and the configuration of the exported POZ, CI and EPO were optimized by B3LYP/6-311++G(2d,2p), Gauss03, and Gauss03W software.

3. Conclusions

We investigated the reaction of ozone with TME in the condensed phase by slowly warming up the matrix sample. During the process, the POZ was successfully observed. According to the optimized calculation results based on B3LYP/6-311++G(2d,2p), the characteristic absorption peaks of POZ are found to be OOO anti-stretching vibration, the coupling peak of C–O stretching vibration and CH_3 bending vibration, and the coupling of CCC and CH_3 bending vibration. The experimental results are consistent with theoretical calculation and previous reports. Nevertheless, the SOZ was not observed in the reaction. Based on the optimized calculation of B3LYP/6-311++G(2d,2p), the strongest peak of SOZ was corresponded to the combination of OCO symmetric stretching vibration, CH_3 bending vibration, and COC antisymmetric stretching vibration. The experimental results after POZ decomposition do not match with the theoretical calculation of SOZ. It is expected that the $(\text{CH}_3)_2\text{COO}$ radical i.e. CI react with TME to form tetramethyl EPO. The experimental spectrum is agreed with the calculation of EPO. The reaction of $^{18}\text{O}_3$ with TME can be further used to verify the formation of EPO. Furthermore, the group 6-311++G(2d,2p) of the B3LYP hybrid function density functional theory method (DFT) was used to optimize the calculation. In contrast, we found that the B3LYP/6-311++G(2d,2p) can accurately predict the intermediate of the reaction. The structure of POZ and tetramethyl epoxypropane is optimized by this method, and the production process of ozone-TME reaction is well presented.

Declaration of competing interest

We declare that we have no financial and personal relationships with other people or organizations that can inappropriately influence our work, there is no professional or other personal interest of any nature or kind in any product, service and/or company that could be construed as influencing the position presented in, or the review of, the manuscript entitled, "Transient Species in the Ozonolysis of Tetramethylethylene".

Acknowledgments

This work was primarily supported by National Key R&D Program of China (No. 2019YFC0214200), National Environmental Protection Public Welfare Industry Research Project (No. 201509010), National Basic Science Research Program of Chinese Research Academy of Environmental Sciences (No. JY-21277132-201309406) and the National Natural Science Foundation of China (No. 21277132).

REFERENCES

- Baley, P.S., Ferrell, T.M., 1978. Mechanism of ozonolysis. A more flexible stereochemical concept. *J. Am. Chem. Soc.* 100 (3), 899–905.
- Chen, J.H., Deng, J.G., Geng, C.M., Yang, X.L., Wang, W., 2013. Reaction mechanism of ozone and propene at low temperatures. *Environ. Chem.* 32 (10), 1827–1833.
- Criegee, R., 1975. Mechanism of ozonolysis. *Angew. Chem. Int. Ed.* 14 (11), 745–752.
- Deng, J.G., Chen, J.H., Geng, C.M., Liu, H.J., Wang, W., Bai, Z.P., et al., 2012b. The overall reaction process of ozone with methacrolein and isoprene in the condensed phase. *J. Phys. Chem. A* 116 (7), 1710–1716.
- Deng, J.G., Chen, J.H., Liu, H.J., Wang, X., 2012a. Matrix isolation FT-IR study on the reaction mechanism of ozone and ethene. *Res. Environ. Sci.* 25 (1), 1–9.
- Epstein, S.A., Donahue, N.M., 2008. The kinetics of tetramethylethene ozonolysis: decomposition of the primary ozonide and subsequent product formation in the condensed phase. *J. Phys. Chem. A* 112 (51), 13535–13541.
- Epstein, S.A., Donahue, N.M., 2010. Ozonolysis of cyclic alkenes as surrogates for biogenic terpenes: primary ozonide formation and decomposition. *J. Phys. Chem. A* 114 (28), 7509–7515.
- Feltham, E.J., Almond, M.J., Marston, G., Vivienne, P.L., Wiltshire, K.S., 2000. Reactions of alkenes with ozone in the gas phase: A matrix-isolation study of secondary ozonides and carbonyl-containing reaction products. *Spectrochim. Acta Part A* 56 (13), 2605–2616.
- Frisch, M.J., Trucks, G.W., Schlegel, H., 2004. Gaussian 03. Gaussian, Inc, Wallingford CT.
- Giorio, C., Campbell, S.J., Bruschi, M., Tampieri, F., Barbon, A., Toffoletti, A., et al., 2017. Online quantification of Criegee intermediates of alpha-pinene ozonolysis by stabilization with spin traps and proton-transfer reaction mass spectrometry detection. *J. Am. Chem. Soc.* 139 (11), 3999–4008.
- Griesbaum, K., Volpp, W., Greinert, R., Greunig, H.J., Schmid, J., Henke, H., 1989. Ozonolysis of tetrasubstituted ethenes, cycloolefins, and conjugated dienes on polyethylene. *J. Org. Chem.* 54 (2), 383–389.
- Hinrichs, T.A., Ramachandran, V., Murray, R.W., 1979. Epoxidation of olefins with carbonyl oxides. *J. Am. Chem. Soc.* 201, 1282–1287.
- Hoffmann, T., Bandur, R., Marggraf, U., Linscheid, M., 1998. Molecular composition of organic aerosols formed in the α -pinene/O₃ reaction: Implications for new particle formation processes. *J. Geophys. Res.* 103 (D19), 25569–25578.
- Hull, L.A., Hisatsune, I.C., Heicklen, J., 1972. Low-temperature infrared studies of simple alkene-ozone reactions. *J. Am. Chem. Soc.* 94 (14), 4856–4864.
- Jani, P.H., Neil, M.D., 2018. Pressure stabilization of Criegee intermediates formed from symmetric trans-alkene ozonolysis. *J. Phys. Chem. A* 122 (49), 9426–9434.
- Jussi, A., Iwona, K., Justyna, K., Jan, L., Maria, W., 2018. FTIR matrix isolation and theoretical studies of glycolic acid dimers. *J. Mol. Struct.* 1163, 294–299.
- Krupa, J., Wierzejewska, M., 2016. Structure of isothiocyanic acid dimers. Theoretical and FTIR matrix isolation studies. *Chem. Phys. Lett.* 652, 46–49.
- Kugel, R.W., Ault, B.S., 2015. Infrared matrix isolation and theoretical studies of reactions of ozone with bicyclic alkenes: alpha-Pinene, norbornene, and norbornadiene. *J. Phys. Chem. A* 119 (2), 312–322.
- Laura, C., Emilie, P., Nicolas, M., Bénédicte, P., Wuyin, Z., Nicolas, M., et al., 2019. Secondary organic aerosol formation from aromatic alkene ozonolysis: Influence of the precursor structure on yield, chemical composition, and mechanism. *J. Phys. Chem. A* 123, 1469.
- Lv, C., Du, L., Tang, S.S., Tsona, N.T., Liu, S.J., Zhao, H.L., et al., 2017. Matrix isolation study of the early intermediates in the analysis of selected vinyl ethers. *RSC Adv.* 7, 19162–19168.
- Murray, R.W., Jeyaraman, R., 1985. Dioxiranes: synthesis and reactions of methyl dioxiranes. *J. Org. Chem.* 50 (16), 2847–2853.
- Niki, H., Maker, P.D., Savage, C.M., Breitenbach, L.P., Hurley, M.D., 1987. FTIR spectroscopic study of the mechanism for the gas-phase reaction between ozone and tetra-methylethene. *J. Phys. Chem.* 91 (91), 941–946.
- Rabi, C.P., Robin, J.S., David, P.T., Rebecca, L.C., Marta, D., Callum, W., et al., 2019. Experimental and computational studies of Criegee intermediate reactions with NH₃ and CH₃NH₂. *Phys. Chem. Chem. Phys.* 21, 14012–14052.
- Rouso, A.C., Hansen, N., Jasper, A.W., Ju, Y., 2019. Identification of the Criegee intermediate reaction network in ethene ozonolysis: impact on energy conversion strategies and atmospheric chemistry. *Phys. Chem. Chem. Phys.* 21 (14), 7341–7357.
- Samuni, U., Haas, Y., Fajgar, R., Pola, J., 1998. Matrix effects in the low-temperature ozonation of ethene, tetramethylethene and 1-hexene. *J. Mol. Struct.* 449, 177–201.
- Sang, W.H., Kwan, K., 1996. Infrared matrix isolation study of acetone and methanol in solid argon. *J. Phys. Chem.* 100 (43), 17124–17132.
- Shama, A., Reva, I., Fausto, R., 2008. Matrix-isolation study and Ab initio calculations of structure and spectra of hydroxyacetone. *J. Phys. Chem. A* 112 (26), 5935–5946.
- Tang, S.S., Du, L., Tsona, N.T., 2017. A new reaction pathway other than the Criegee mechanism for the ozonolysis of a cyclic unsaturated ether. *J. Atmos. Env.* 162, 23–30.
- Wang, Z.P., Yuri, A.D., Bu, Y.X., 2019. Dynamics insight into isomerization and dissociation of hot Criegee intermediate CH₃CHOO. *J. Phys. Chem. A* 123 (5), 1085–1090.